Investigating the effect of land use changes on soil erosion using RS-GIS and AHP-Fuzzy based techniques (Case Study: Qaresu Watershed, Ardabil, Iran)

Investigación del efecto de los cambios en el uso de la tierra en la erosión del suelo utilizando técnicas basadas en RS-GIS y AHP-Fuzzy (Estudio de caso: Qaresu Watersu, Ardabil, Irán)

Fereshteh Namdar[1], Shahla Mahmoudi[2,*], Abazar Esmali Ouri[3], Ebrahim Pazira[1]

[1] Department of Soil Science, Science and Research Branch, Islamic Azad University, Tehran, Iran.
[2] Department of Soil Science, University of Tehran, Tehran, Iran.
[3] Department of Natural Resources, University of Mohaghegh Ardabili, Ardabil, Iran.

*Corresponding autor email: smahmodi@ut.ac.ir

ABSTRACT

The intensity of soil erosion to occur in a region depends on multiple factors including climatic conditions, elevation, terrain, soil type, and land use. Among these factors, land use is one of the particular importance as it reflects the outsized role of humans in the exacerbation of erosion condition. This study aimed to investigate the effects of land use changes on soil erosion in Qaresu watershed, using Remote Sensing (RS) and Geographical Information System (GIS) techniques, a watershed with an area of 4370.8 km² located in the center of Ardabil province, northwest of Iran. For this purpose, the 1985 and 2015 Landsat images captured by TM and OLI-TIRS sensors were used to develop the land use maps of the watershed area using the maximum likelihood method. The erosion zoning maps were then developed by integrating the maps of land use, slope, lithology, distance from roads, distance from streams, precipitation, and soil using the Weighted Linear Combination (WLC) method after an AHP-based weighting stage. The results showed that in the 30-year period from 1985 to 2015, the region has experienced a decrease in the area of forest, dry farming, and rangeland land uses and an increase in the area of land uses defined as urban, barren, irrigated farming, and water cover. In total, dry farming and rangeland were the largest land-uses in the studied area. According to the developed erosion zoning maps, in 1985, 14.4% and 36.84%, and in 2015, 15.64% and 32.3% of the studied area belonged to high and very high risk zones in terms of erosion potential, respectively. In defined two periods, high risk and very high risk zones were mostly positioned over dry and irrigated farmlands.

Keywords: Fuzzy Logic, Land Use, Maximum Likelihood, Water Erosion, Weighted Linear Combination.

RESUMEN

La intensidad de la erosión del suelo que se producirá en una región depende de múltiples factores, incluidas las condiciones climáticas, la elevación, el terreno, el tipo de suelo y el uso del suelo. Entre estos factores, el uso de la tierra es uno de particular importancia, ya que refleja el enorme papel de los seres humanos en la exacerbación de la condición de erosión. Este estudio tuvo como objetivo investigar los efectos de los cambios de uso de la tierra en la erosión del suelo en la cuenca hidrográfica de Qaresu, utilizando técnicas de Teledetección (RS) y Sistema de Información Geográfica (GIS), una cuenca hidrográfica con un área de 4370,8 km2 ubicada en el centro de la provincia de Ardabil, noroeste de Irán. Para este propósito, las imágenes Landsat de 1985 y 2015 capturadas por los sensores TM y OLI-TIRS se utilizaron para desarrollar los mapas de uso del suelo del área de la cuenca utilizando el método de máxima verosimilitud. Los mapas de zonificación de erosión se desarrollaron integrando los mapas de uso de la tierra, pendiente, litología, distancia de las carreteras, distancia de los arroyos, precipitación y suelo utilizando el método de combinación lineal ponderada (WLC) después de una etapa de ponderación basada en AHP. Los resultados mostraron que en el período de 30 años de 1985 a 2015, la región ha experimentado una disminución en el área de bosques, cultivos de secano y pastizales y un aumento en el área de usos de la tierra definidos como urbanos, estériles, irrigados. agricultura y cobertura de agua. En total, la agricultura de secano y los pastizales fueron los usos más importantes de la tierra en el área estudiada. De acuerdo con los mapas de zonificación de erosión desarrollados, en 1985, 14,4% y 36,84%, y en 2015, 15,64% y 32,3% del área estudiada pertenecía a zonas de alto y muy alto riesgo en términos de potencial erosivo, respectivamente. En dos períodos definidos, las zonas de alto riesgo y muy alto riesgo se ubicaron principalmente sobre tierras agrícolas secas y de regadío.

Palabras clave: lógica difusa, uso del suelo, probabilidad máxima, erosión hídrica, combinación lineal ponderada.

1. INTRODUCTION

Land use change is widely accepted as an important determinant of erosion trends that its effects have directly affected erosion (Dadashpoor et al. 2019; Namugize et al. 2018; Pham et al. 2018). Given the critical role of land use in erosion, land use studies can serve as a guide on how to maintain or restore the balance of an ecosystem (NazariSamani et al. 2010; Sun and Li 2017). Typically, land use changes are identified by tracking altered areas in images captured from the same area at different periods (Sui 1999). The use of Remote Sensing (RS) and Geographical Information System (GIS) is most important way for this purpose (Imran Basha et al. 2018; Siddi Raju et al. 2018). Satellite imagery is particularly suitable for this application as it can provide a wide variety of up-to-date digital information (Rajasekhar et al. 2018; Zohaib et al. 2019) that can be processed into land use maps. Thanks to these features, RS data and GIS environment can give us a good understanding of how land uses are changing and help us devise fitting management solutions to mitigate or counter the consequent problems (Coppin et al. 2004; Mendoza 2004).

Many developing countries suffer from soil erosion problems, but this issue has reached a particularly grave situation in Iran (Arekhi et al. 2012).With the growing rate of soil erosion in the past century, it has become one of the leading environmental problems that threaten agriculture and natural resources in Iran as well as many other countries (Alkharabsheh et al. 2013; Rahman et al. 2009). Soil erosion is controlled by several factors including climatic conditions, elevation, soil type, and land use (Ochoa et al. 2016; Wang et al. 2016). Among these factors, rainfall and land use are more dynamic and are also more affected by human activities (Keesstra et al. 2016; Mekonnen et al. 2015). The present study concludes that human activities, which are reflected in land use, have a significant impact on erosion (Palazon and Navas 2016).

The impacts of vegetation and land use on erosion in different parts of the world have been extensively researched (Santos et al. 2017; Xiao et al. 2015). The studies in this area have shown that under certain conditions, these two factors can have a positive impact on soil erosion. Many of these studies have reported that soil erosion is significantly affected by the type of cultivation, particularly shifting cultivation, and agricultural activities in general (Garca-Ruiz 2010; Latocha et al. 2016; Nunes et al. 2011). Also, many studies in this area have shown the significant impact of vegetation on soil erosion (Anh et al. 2014; Ferreira and Panagopoulos 2014; Li et al. 2014; Mohammad and Adam 2010; Wang et al. 2016).

Tracking land use changes and assessing their impact on erosion are among the primary perquisites for comprehensive management of watersheds. The area studied in this work is the Qaresu watershed located in Ardabil province, Iran. The objective of this study was to investigate the effects of land use changes over the last thirty years on the soil erosion in this watershed, in order to facilitate land use management and soil erosion control decision-making for this area.

Preparation of land use change maps in 30 years with high accuracy and investigating its effects on soil erosion using RS-GIS and AHP-Fuzzy based techniques is a new study in this region with 4370.8 km² area which is of great importance for the region because of its extent and role in the local economy.

2. MATERIAL AND METHODS

2.1. Study Area

Qaresu watershed is the largest and most important watershed of Ardabil province, Iran. This watershed is located at the center of Ardabil province between $47°48'10''$-$48°41'50''$ Eastern longitudes $37°46'27''$-$38°35'10''$ Northern latitudes and covers an area of 4370.8 km² across three counties of Ardabil, MeshginShahr and Namin. This watershed has a maximum altitude of about 3700 meters in the west and drains into the Sabalan Dam in the north at an altitude of about 1200 meters (Bureau of Natural Resources and Watershed Management of Ardabil Provence 2018). The location of Qaresu watershed in Ardabil province is displayed in Fig. 1.

2.2. Research Data

The present study was an applied research conducted with an analytical approach based on the integration of data analysis and RS-GIS techniques. After preparing the digital layers of the Qaresu watershed area, the 1:50,000 topographic map of the area was used to determine, for each point, the distance from streams and roads and the slope percentage, which has been drawn before 1985. The soil and geological maps of the study area were extracted from the 1:100,000 soil and geological maps of the Geological and Soil Research Center of Ardabil province. Since the changes in soil class and geological units over a 30-year period from 1985 to 2015 are negligible, the same map is used for both years. The precipitation map was prepared using the data of Ardabil, Nir, Namin, MeshginShahr meteorological stations and their adjacent meteorological stations by Inverse Distance Weighting (IDW) interpolation. The land use maps were prepared based on the official land use map of the province, Google Earth images, field surveys, Landsat 8 satellite images (OLI-TIRS path 165 row 35 taken in 2015) and Landsat 5 satellite images (TM path 165 row 35taken in 1985). These criteria were chosen after reviewing similar articles and the factors that influence erosion in the region of interest and determining whether relevant data layers can be acquired. Regarding geological and soil factors, it must be explained that given the expanse of the region, it contains several geological formations and soil classes which naturally create different erosion potentials in different parts. Proximity to roads increases soil erosion due to construction activities. Steep slopes, rainfalls, and water streams all facilitate the transport of soil particles, which translates into increased erosion. Land use also has a notable impact on soil erosion through its influence on soil characteristics and

vegetation. The software applications ArcGIS 10.4.1, Erdas Imagine 2014, Envi 5.3, and Excel 2016 were used for data processing and analysis.
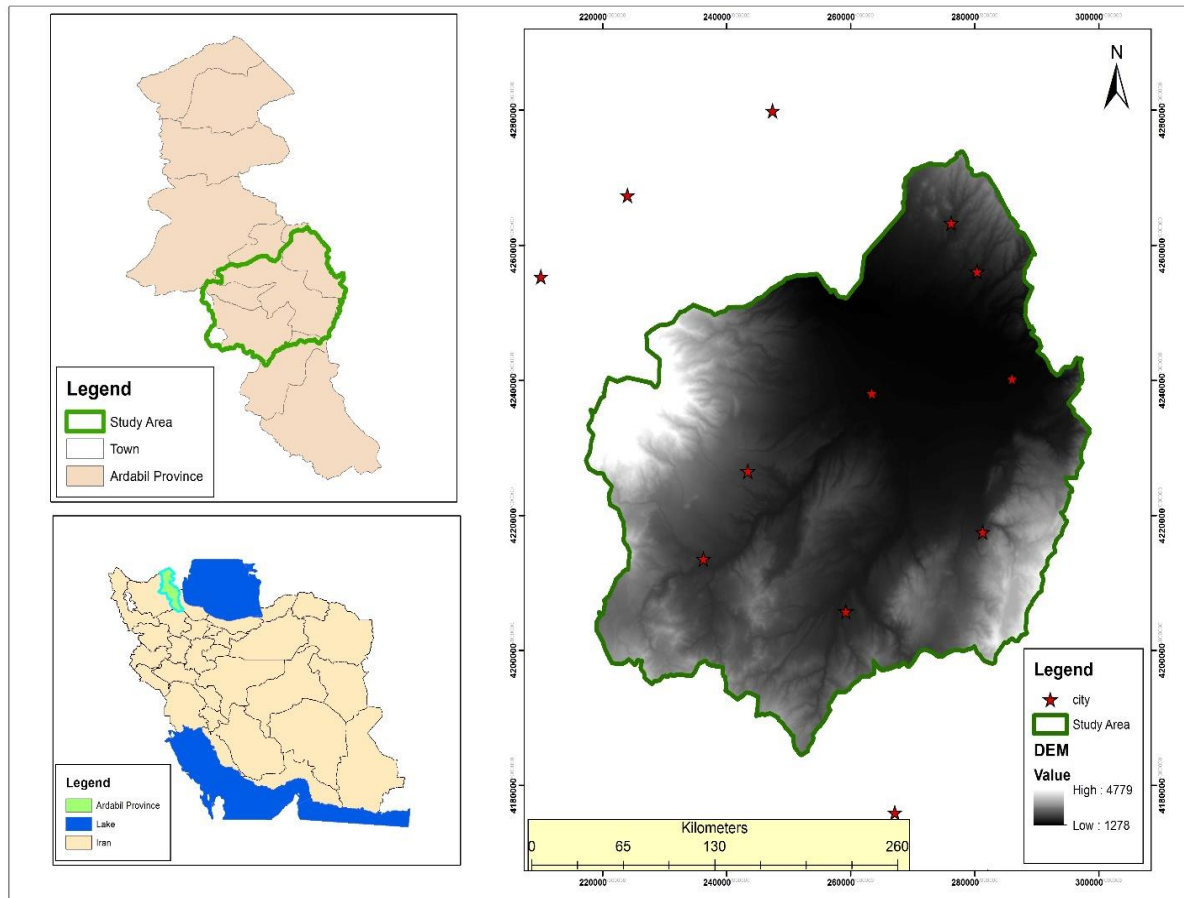

Figure 1. Location of the studied area

2.3. Methodology

The acquired satellite images underwent a pre-processing stage consisting of geometric, radiometric and elevation corrections. For geometric correction, Landsat 8 images were overlaid on the stream and road layers extracted from the topographic map. This comparison showed a good agreement, indicating that the image has no geometric error. For 1985 images, the geometric correction was performed using the image-to-image method with RMS = 0.14. The radiometric correction was carried out using the Chavez method. Given the high elevation difference and partly mountainous terrain of the area, topographic normalization was performed using the Minnaert method (Equation 1) and the Digital Elevation Model (DEM) based on sun elevation and azimuth values obtained from the text file attached to images.

$$BVnormal\lambda = \frac{\text{BVobserved}\lambda \text{ COS e}}{\text{K} (\cos i) (\cos e)}$$

(1)

Where, BV_{normal} denotes the normalized brightness values, $BV_{observed}\lambda$ the observed brightness values, cos i the cosine of the incidence angle, cos e the cosine of the slope angle, and K the Minnaert constant (Aslami

528

et al. 2015). Next, land use maps of each year (1985 and 2015) were developed by band combination of the images using the Maximum Likelihood Classification method (a supervised classification method) based on the training samples obtained for each land use from the field survey. Field surveys showed that there are no dry land farms on the slopes steeper than 30%. Therefore, these lands must be considered poorly vegetated rangelands and are classified as such to increase precision. So the slope of 30% was used as the threshold for differentiating rangelands from dry farms. The NDVI layer was also used to better distinguish barren lands from sparsely vegetated rangelands. To evaluate the classification accuracy, the Kappa statistic was calculated using Equation 2. This statistic can be considered a good metric for evaluating the accuracy of this classification as it also takes into account the incorrectly classified pixels.

$$k = \frac{p_0 - p_c}{1 - p_0}$$

(2)

Where, Po is the observed agreement and Pc is the chance expected agreement. The ideal value for kappa statistic is 1. A kappa statistic that is closer to zero indicates the higher randomness of the classification and negative kappa values signify erroneous classification (Arekhi et al. 2012).

Finally, the soil erosion zoning maps pertaining to the years 1985 and 2015 were developed by integrating lithology, soil, slope, distance from roads, distance from streams, land use, and precipitation layers using the Weighted Linear Combination (WLC) after an AHP[1]-based weighting stage. The flowchart of the research procedure is illustrated in Fig. 2.
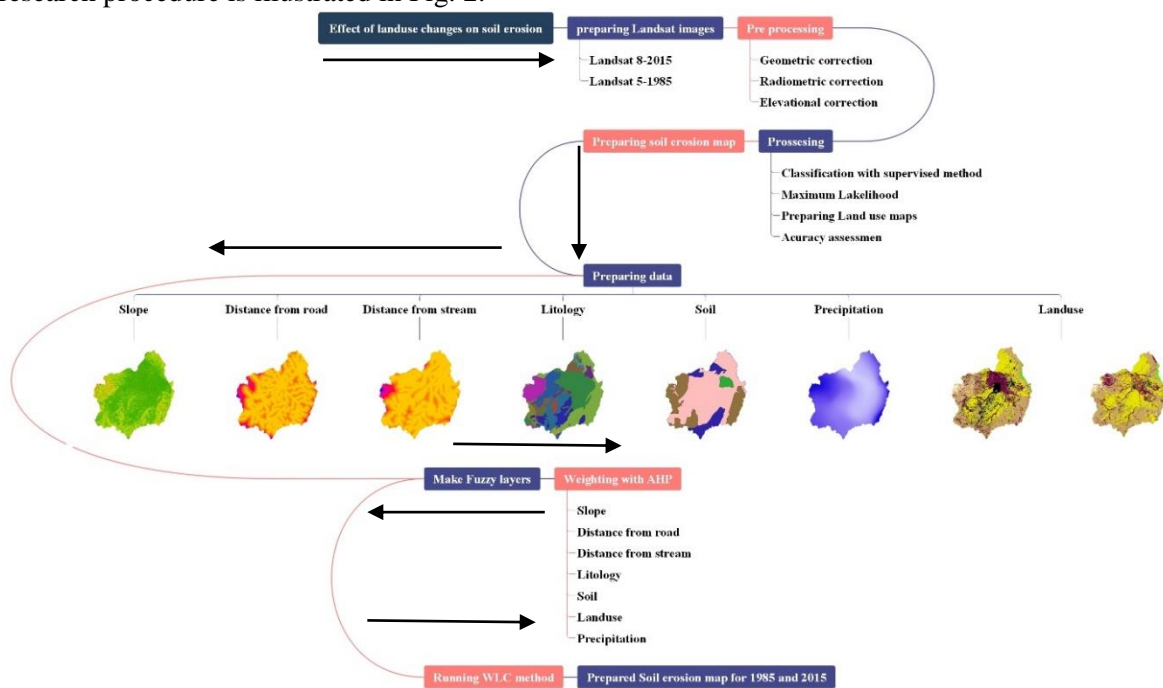

Figure 2. Flowchart of research procedure

The information related to the parameters used in this study is illustrated in Fig. 3.
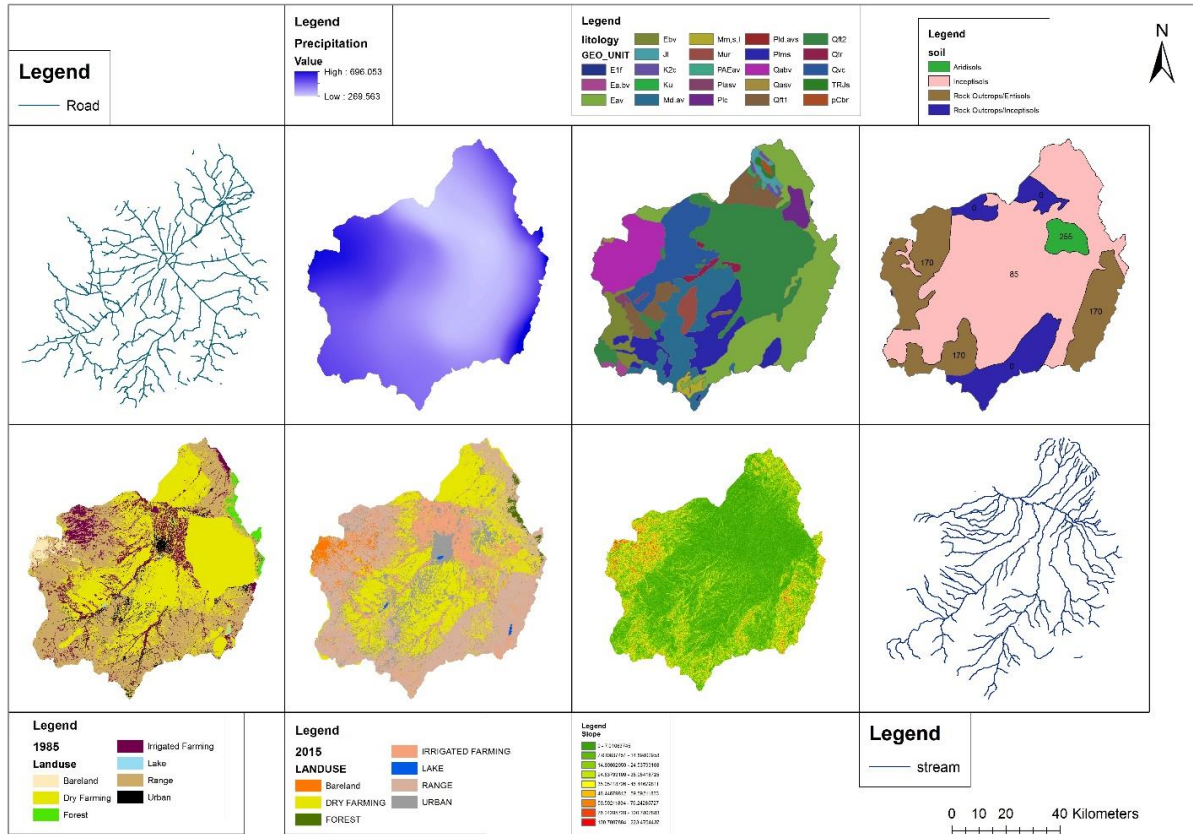
---

[1] Analytic Hierarchy Process

Figure 3. The information related to the parameters used in this study

Roads: This includes primary roads and has been extracted from the 1:50000 topographic map of the province.

Precipitation: Precipitation maps obtained from the interpolation models shows that the minimum and maximum precipitation in the region are 269mm and 696mm, with the lowest precipitation occurring in the central parts and highest in the western parts.

Geology: The geological map shows that the region contains 23 types of geological units of different sizes, which are extensively dispersed over the region. The largest geological unit in the region is Qft2.
Soil class: There are a total of four soil classes in the region, the largest of which is Inceptisol covering most of the northern, central, and southern parts.

Land use: Land use maps prepared using the supervised classification method show that in both years (1985 and 2015) most of the region has been covered with rangelands and dry land farms.

Slope: The slope map derived from the Digital Elevation Model (DEM) shows that most of the region has a flat terrain with a maximum slope of less than 5%. Slopes of more than 10% can be found only in the western and eastern parts of the region

Water streams: The region has two major water streams, Baliqly-Chay River and Ghareh-Su River, which flow into Sabalan Dam in the west of the region.

2.4. Weighted Linear Combination (WLC)

530

Before initiating the WLC procedure, every map had to be standardized. In this study, a fuzzy method was used for standardization. In fuzzy sets, membership of an item in a set is expressed not by binary values but by a degree of membership, which ranges from 0 representing minimum or no membership to 1 representing the maximum or full membership. In other words, the highest degree of membership is given a value of 1 and the lowest is given a value of zero (Sui 1999). The weight of each criterion was obtained using the CRITIC[2]weighting method. In this method, data are weighted based on the degree of correlation and conflict between factors or criteria. In the fuzzy form of the CRITIC method, the range of variations of measured values in pixels (alternatives) with respect to each criterion is expressed by a membership function. For each criterion, a vector must be formed to compute the standard deviation of the value of factor over the studied alternatives. After calculating the standard deviations for all factors and criteria, a symmetrical m×m matrix consisting of coefficients of correlation between formed vectors must be created. After completing the above procedures, the conflict of criterion j with other criteria must be calculated by Equation 3.

$$\text{Cjk} = \sum_{k=1}^{m} 1 - rjk$$

(3)

Where, Cjk is the sum of conflict of criterion j with criteria k (from k = 1 to k = m), and rjk is the correlation between the criteria j and k. The value of information of criterion j is quantified by Equation 4.

$$\text{Cj} = \delta j \sum_{k=1}^{m} 1 - rjk$$

(4)

Where, Cj represents the value of information of criterion j and it is the standard deviation in the values of the factor or criterion j. According to the above relationships, the criteria with higher Cj values will be given a higher weight. The weight of factor j is determined by Equation 5.

$$Wj = \frac{Cj}{\sum_{k=1}^{m} Ck}$$

(5)

Where, Wj is the weight of the criterion j and Ck represents the total value of information of the criteria k (from k = 1 to k = m). The use of CRITIC method for weighing helps us address the problem of independence of attributes, which if left unchecked, interferes in the pairwise comparison stage of the AHP procedure, leading to underweighting of the criteria that highly correlate with others.

Next, the standardized layers should be multiplied by the corresponding weight to create the weighted standardized layers, which must then be subjected to common overlay operation to determine the score related to each alternative (pixel). After ranking the alternatives in terms of their total score, the alternative with the highest score (rank) should be selected as the best alternative. The score of alternative Ai in this evaluation is given by Equation 6.

$$A_i = \sum_J W_J X_{IJ}$$

(6)

Where, X_{IJ} represents the score of alternative i with respect to attribute j and W_J is a standardized weight. This weight should be normalized so that all weights sum up to one ($\sum w_j = 1$). These weights represent the

---

[2]Importance Through Inter-criteria Correlation

relative importance of attributes. After identifying the maximum value of i = Aj, the most preferred alternative can be determined (Malczewski 2006).

3. RESULTS

After the supervised classification of the studied area, the land use maps for the years 1985 and 2015 were developed based on seven classes: urban, lake, forest, dry farming, irrigated farming, barren, forest, and rangeland (Fig. 4).
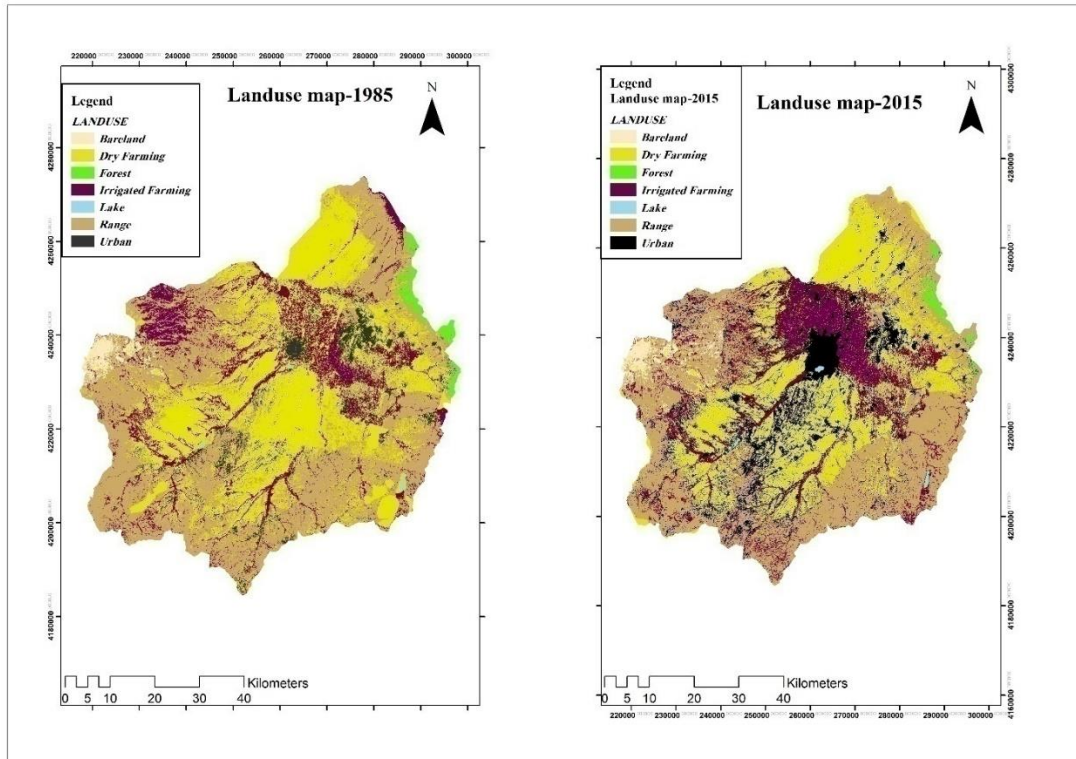
Figure 4. Land use maps of the studied are in 1985 and 2015 (with supervised classification)

3.1. Classification Accuracy

In the accuracy assessment stage, the Kappa statistic of the land use maps obtained for 1985 and 2015 was calculated to 86% and 94%, respectively, which show acceptable classification accuracy. The obtained statistics also indicate that satellite imagery can produce land use maps with acceptable precision (Table 1).

Table 1. Results of the accuracy assessment of land use maps for 1985 and 2015 (in percent)

No.	Land use	User Accuracy		Classification Accuracy	
		2015	1985	2015	1985
1	Irrigated Farming	95.76	75.78	96.05	88.41
2	Rangeland	91.00	87.75	98.42	95.81
3	Forest	97.09	94.91	97.61	89.69
4	Dry Farming	99.18	91.52	93.72	82.51
5	Urban	96.05	97.42	90.12	86.27
6	Barren	92.02	90.01	89.19	85.54
7	Lake	92.11	91.08	88.14	86.72
1985	Kappa			86	
	Overall accuracy			90.06	
2015	Kappa			94	
	Overall accuracy			95.60	

3.2. Land Cover Changes

According to the land use map developed for 1985, at that time, dry farming with a surface area of 2011.3 km^2, rangeland with an area of 1635.58 km^2, and irrigated farming with an area of 478.03 km^2 were the largest land uses in the region. As can be seen, the smallest land uses in that year were urban, barren, forest and lake in that order. According to the 2015 land use map, rangeland with a surface area of 1591.50 km^2, dry farming with a surface area of 1445.41 km^2, and an irrigated farming with a surface area of 625.13 km^2 are still the largest land uses in the area, and urban, barren, forest and lake are still the smallest land uses (Table 2). However these results also show an increase in the area of irrigated farming, urban, barren and lake land uses and a decrease in the area of dry farming, rangeland, and forest land uses in the region.

Table 2. Area (km^2), percentage share, and change of land use in Qaresu watershed for the 1985-2015 period

No.	Land use class	Year						Trend
		1985		2015		Change		- / +
		Area (km^2)	Percentage	Area (km^2)	Percentage	Area (km^2)	Percentage	
1	Dry Farming	2011.33	46.02	1445.41	33.07	565.92	12.95	-
2	Forest	50.36	1.15	32.40	0.74	17.96	0.41	-
3	Irrigated Farming	478.03	10.93	625.13	14.30	147.1	3.37	+
4	Rangeland	1635.58	37.42	1591.50	36.41	44.08	1.01	-
5	Urban	132.05	3.02	572.84	13.10	440.79	10.08	+
6	Barren	58.11	1.32	96.35	2.20	38.24	0.88	+
7	Lake	4.90	0.11	6.74	0.15	1.84	0.04	+

3.3. Soil Erosion Zoning

For soil erosion zoning, first, the weight of criteria was determined using the CRITIC weighting method. The basic assumptions used for the CRITIC weighing of criteria and the weights derived from this method are provided in Table 3. It should be noted that besides land use, we also observed changes in other factors such as precipitation over the study period, and given the mutual effects of these factors on each other in

determination of weight, this affects the weights of these factors. The procedure of the WLC method was then followed to develop two erosion zoning maps consisting of five zones (very high risk, high risk, moderate risk, low risk, and very low risk) for the years 1985 and 2015 (Fig. 5). The total area of each zone in each map is also provided in Table 4.

Table 3. Total conflict, standard deviation, information value, and final weight of the criteria for erosion zoning

|	Criterion	Total conflict	Standard deviation	Information value	Final weight
Based on 1985 land use map	Slope	3.584	0.289	1.037	0.152
	Lithology	2.632	0.402	1.058	0.155
	Land use	2.804	0.401	1.126	0.165
	Soil	2.291	0.441	1.010	0.148
	Precipitation	2.781	0.372	1.036	0.152
	Distance from streams	1.755	0.434	0.762	0.111
	Distance from roads	1.976	0.391	0.773	0.113
Based on 2015 land use map	Slope	3.584	0.289	1.037	0.161
	Lithology	2.632	0.402	1.058	0.164
	Land use	2.641	0.362	0.957	0.148
	Soil	2.165	0.441	0.955	0.148
	Precipitation	2.701	0.372	1.006	0.156
	Distance from streams	1.627	0.434	0.706	0.109
	Distance from roads	1.841	0.391	0.720	0.111
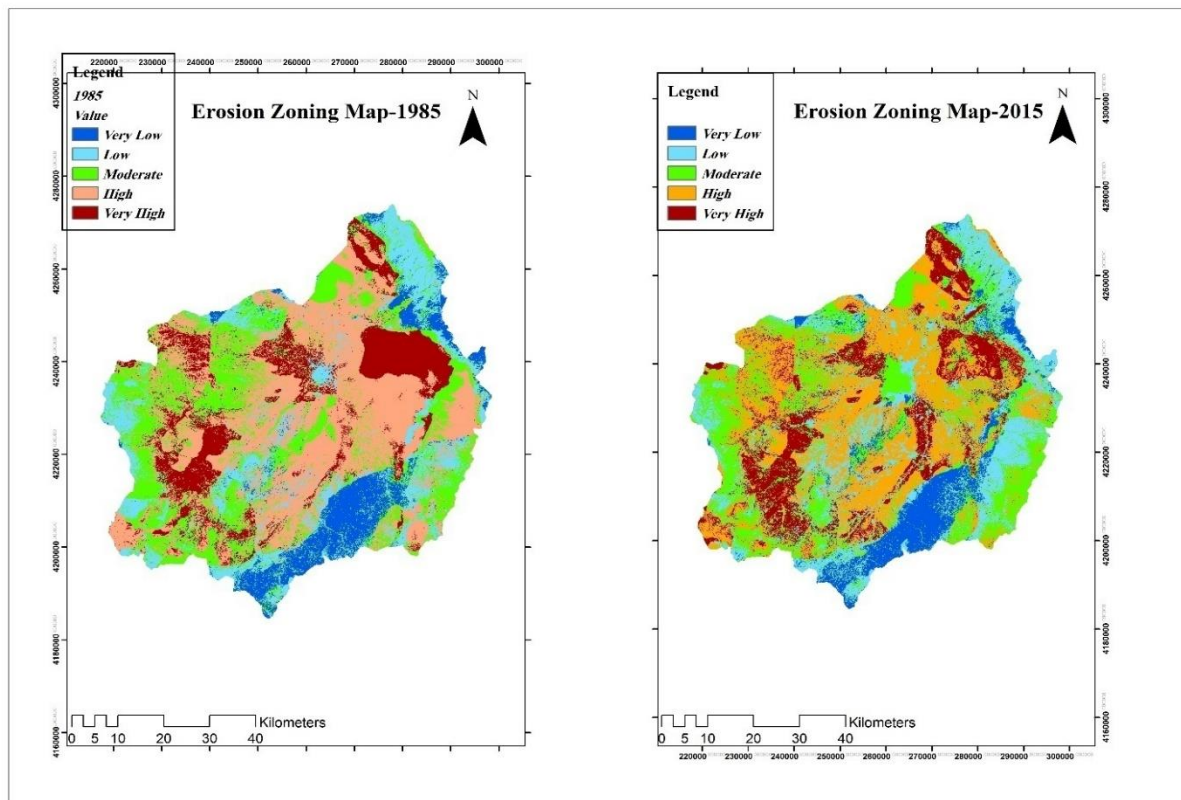
Figure 5. Erosion zoning maps of the studied area for 1985 and 2015 (from the WLC method)

534

Table 4. Area (km²) and percentage share of erosion risk zones in Qaresu watershed for 1985 and 2015 (from the WLC method)

| No. | Erosion Zone | Year | | | | Change | | Trend +/- |
| | | 1985 | | 2015 | | | | |
		Area (km²)	Percentage	Area (km²)	Percentage	Area (km²)	Percentage	
1	Very High Risk	631.22	14.4	683.14	15.64	51.92	1.24	+
2	High Risk	1608.6	36.84	1410.32	32.3	198.28	4.54	-
3	Moderate Risk	1069.76	24.5	1031.8	23.6	37.96	0.9	-
4	Low Risk	681.51	15.61	868.99	19.90	187.48	4.29	+
5	Very Low Risk	379.39	8.57	376.28	8.50	3.11	0.07	-

4. DISCUSSION AND CONCLUSION

In this study, land use maps of the area of interest for the years 1985 and 2015 were prepared by supervised classification of the area into seven classes. The investigation of land use changes in the area shows that from 1985 to 2015, the area under irrigated farming has increased by 147.1 km². This increase can be attributed to the fact that a large portion of the Qaresu watershed is positioned in the Ardabil plain, which makes it easier to transform dry farms and rangelands to irrigated farms by digging wells and tapping into ground waters. This trend itself is a notable environmental threat and is likely to cause a steady reduction in groundwater levels and eventually ground subsidence. Even now, there are some signs of subsidence in several parts of the region that are under irrigated cultivation. The results show a 440.79 km² increase in the area of urban land uses in the region, which is a result of population growth and consequent expansion of construction activities. This expansion has resulted in the absorption of dry farmlands into urban zones to provide the space needed for the growth of cities. Because of this need, developers have been successful in purchasing dry farms adjacent to existing residential areas and acquiring the necessary permits to convert them, along with nearby rangelands and irrigated farms, into houses and apartments. In general, the primary cause of the 565.92 km² reductions in the area of dry farmlands and 44.08 km² reductions in the area of rangelands is their conversion into irrigated farmlands and urban land uses. In some parts of the region, the high quality of soil, favorable weather conditions, and socioeconomic factors have stimulated the conversion of rangelands into farmland. But because of the steep slope of these rangelands and reduced precipitation of recent years, many of these new farms have been abandoned to gradually turn into sparsely vegetated and eventually barren lands. This is the reason behind the 38.24 km² increase in the area of barren lands. The reason for 1.84 km² increase in the area of water cover (lake land use) in the region is the construction of Saghezchi and Sabalan dams. Another noticeable change in the region is the degradation of vegetation through the replacement of forest with rangelands because of illicit logging activity in Fandoghlu forests, which is reflected in the 17.96 km² reductions in the area of forest land use in the region.

The erosion zoning maps obtained for both 1985 and 2015 show that the areas with high and very high risk of erosion are mainly positioned in lake, dry farming, and barren land uses, the areas with very low risk of erosion are dominantly located in forest and rangeland land uses, and the areas with low and moderate risk of erosion are mostly in rangeland and urban land uses. These results are consistent with the results of Da Silva et al. (2016), Esfandiari et al. (2014), Feizizadeh (2017) and Martnez-Murillo et al. (2011) which have reported that forests, rangelands, barren lands, dry farmlands, and irrigated farmlands

have the lowest potentials for erosion in that order. As the results presented in Table 4 indicate, from 1985 to 2015, there has been an increase in the area of very high and low risk zones and a decrease in the area of high risk, moderate risk and very low risk zones. During this period, there has been a 198.28 km^2 decreases in the area of high risk zone and 37.96 km^2 reduction in the area of moderate risk zone, which can be attributed to the transformation of these lands into very high risk zones. This is reflected in the 51.92 km^2 increase in the area of very high risk zone due to the increased area of barren lands (by 38.24 km^2), irrigated farmlands (by 147.1 km^2) and the decreased area of rangelands (by 44.08 km^2). In this respect, the results are similar to the findings of Martnez-Murillo et al. (2011), which highlight the role of vegetation and intact natural landscapes (undisturbed of cultivation) on erosion control. The second cause of the observed reduction in the area of high risk zone is the conversion of farmlands to low risk residential areas, which is reflected in the 440.79 km^2 increase in the area of urban land uses and the 187.48 km^2 increase in the area of low risk zones. However, another cause of the increase in the area of low risk zones is the 17.96 km^2 reduction in the area of forests and the consequent conversion of very low risk areas to low risk. This finding underscores the significant impact of forests on the extent of erosion in the region.

Given the observed trends, the studied area seems to be in urgent need of new measures within the framework of environmental protection programs with the objective of preserving natural landscapes and preplanning, stabilization, and legal enforcement of land uses especially in areas with high risk of erosion. The preparation and reexamination of cadastral maps for differentiating public lands from farmlands can also contribute to the development of a master map with the purpose of preventing illicit or fraudulent land use change. Another recommendation is the commitment to biological operations such as seedling and restoration planting and conversion of low productivity dry farms to rangelands in order to enhance the vegetation cover, although this requires careful ecological capability evaluations and adoption of a well-disciplined land-use planning procedure in the region.

REFERENCES

Alkharabsheh, M. M., Alexandridis, T. K., Bilas, G., Misopolinos, N., & Silleos, N. (2013). Impact of land cover change on soil erosion hazard in northern Jordan using remote sensing and GIS. Procedia Environmental Sciences, 19, 912-921.

Anh, P. T. Q., Gomi, T., MacDonald, L. H., Mizugaki, S., Van Khoa, P., & Furuichi, T. (2014). Linkages among land use, macronutrient levels, and soil erosion in northern Vietnam: a plot-scale study. Geoderma, 232, 352-362.

Arekhi, S., Darvishi, A., Shabani, A., Fathizad, H., & Ahmadai Abchin, S. (2012). Mapping soil erosion and sediment yield susceptibility using RUSLE, remote sensing and GIS (Case study: Cham Gardalan Watershed, Iran). J. Adv. Environ. Biol, 6(1), 109-124.

Aslami, F., Ghorbani, A., Sobhani, B., & Panahandeh, M. (2015). COMPARING ARTIFICIAL NEURAL NETWORK, SUPPORT VECTOR MACHINE AND OBJECT-BASED METHODS IN PREPARATION LAND USE/COVER MAPSUSING LANDSAT-8 IMAGES.

Bureau of Natural Resources and Watershed Management of Ardabil Provence (2018) Reports on the master study of Qaresu watershed in Ardabil.

Coppin, P., Jonckheere, I., Nackaerts, K., Muys, B., & Lambin, E. (2004). Review ArticleDigital change detection methods in ecosystem monitoring: a review. International journal of remote sensing, 25(9), 1565-1596.

Dadashpoor, H., Azizi, P., & Moghadasi, M. (2019). Land use change, urbanization, and change in landscape pattern in a metropolitan area. Science of The Total Environment, 655, 707-719.

Da Silva, V. D. P., Silva, M. T., & Souza, E. P. D. (2016). Influence of land use change on sediment yield: a case study of the sub-middle of the São Francisco River basin. Engenharia Agrícola, 36(6), 1005-1015.

Esfandiari M, Moini A, Moghaddasi R (2014) Effect of land use and vegetation cover on erosion and sediment production: a case study Varas River Watershed in Qazvin province. Territory Quarterly 11(42):51-62.

Feizizadeh, B. (2017). Modeling the Trends of the Land Use/Cover Change and Its Impacts on the Erosion System of the Allavian Dam Based on the Remote Sensing and GIS Techniques. Hydrogeomorphology, 3(11), 21-38.

Ferreira, V., & Panagopoulos, T. (2014). Seasonality of soil erosion under Mediterranean conditions at the Alqueva dam watershed. Environmental management, 54(1), 67-83.

García-Ruiz, J. M. (2010). The effects of land uses on soil erosion in Spain: a review. Catena, 81(1), 1-11.

Basha, U. I., Suresh, U., Raju, G. S., Rajasekhar, M., Veeraswamy, G., & Balaji, E. (2018). Landuse and Landcover Analysis Using Remote Sensing and GIS: A Case Study in Somavathi River, Anantapur District, Andhra Pradesh, India. Nature Environment and Pollution Technology, 17(3), 1029-1033.

Keesstra, S. D., Bouma, J., Wallinga, J., Tittonell, P., Smith, P., Cerdà, A., ... & Fresco, L. O. (2016). The significance of soils and soil science towards realization of the United Nations Sustainable Development Goals. Soil.

Latocha, A., Szymanowski, M., Jeziorska, J., Stec, M., & Roszczewska, M. (2016). Effects of land abandonment and climate change on soil erosion—An example from depopulated agricultural lands in the Sudetes Mts., SW Poland. Catena, 145, 128-141.

Li, Q., Yu, P., Li, G., Zhou, D., & Chen, X. (2014). Overlooking soil erosion induces underestimation of the soil C loss in degraded land. Quaternary International, 349, 287-290.

Malczewski, J. (2006). GIS-based multicriteria decision analysis: a survey of the literature. International journal of geographical information science, 20(7), 703-726.

Martínez-Murillo, J. F., López-Vicente, M., Poesen, J., & Ruiz-Sinoga, J. D. (2011). Modelling the effects of land use changes on runoff and soil erosion in two Mediterranean catchments with active gullies (South of Spain). Landform Analysis, 17, 99-104.

Mekonnen, M., Keesstra, S. D., Baartman, J. E., Ritsema, C. J., & Melesse, A. M. (2015). Evaluating sediment storage dams: structural off-site sediment trapping measures in northwest Ethiopia. Cuadernos de investigación geográfica, 41(1), 7-22.

Mendoza, M. E., Granados, E. L., Geneletti, D., Pérez-Salicrup, D. R., & Salinas, V. (2011). Analysing land cover and land use change processes at watershed level: a multitemporal study in the Lake Cuitzeo Watershed, Mexico (1975–2003). Applied Geography, 31(1), 237-250.

Mohammad, A. G., & Adam, M. A. (2010). The impact of vegetative cover type on runoff and soil erosion under different land uses. Catena, 81(2), 97-103.

Namugize, J. N., Jewitt, G., & Graham, M. (2018). Effects of land use and land cover changes on water quality in the uMngeni river catchment, South Africa. Physics and Chemistry of the Earth, Parts A/B/C, 105, 247-264.

Nazari Samani, A. A, Ghorbani, M., & Kohbanani, H. R. (2010) Evaluation of land use change trends in Taleghan watershed from 1987 to 2001. Journal of Rangeland, 4(3):442-451.

Nunes, A. N., De Almeida, A. C., & Coelho, C. O. (2011). Impacts of land use and cover type on runoff and soil erosion in a marginal area of Portugal. Applied Geography, 31(2), 687-699.

Ochoa, P. A. A., Fries, A., Mejia, D., Burneo, J. I., Ruíz-Sinoga, J. D., & Cerdà, A. (2016). Effects of climate, land cover and topography on soil erosion risk in a semiarid basin of the Andes. Catena, 140, 31-42.

Palazón, L., & Navas, A. (2016). Land use sediment production response under different climatic conditions in an alpine–prealpine catchment. Catena, 137, 244-255.

Pham, T. G., Degener, J., & Kappas, M. (2018). Integrated universal soil loss equation (USLE) and Geographical Information System (GIS) for soil erosion estimation in A Sap basin: Central Vietnam. International Soil and Water Conservation Research, 6(2), 99-110.

Rahman, M. R., Shi, Z. H., & Chongfa, C. (2009). Soil erosion hazard evaluation—an integrated use of remote sensing, GIS and statistical approaches with biophysical parameters towards management strategies. Ecological Modelling, 220(13-14), 1724-1734.

Rajasekhar, M., Sudarsana, R. G., Siddi, R. R., Padmavathi, A., & Balaram, N. B. (2018). Landuse and Landcover Analysis using Remote Sensing and GIS: A Case Study in Parts of Kadapa District, Andhra Pradesh, India. Journal of Remote Sensing and GIS, 9(3), 1-7.

Santos, J. C. N. D., Andrade, E. M. D., Medeiros, P. H. A., Guerreiro, M. J. S., & Palácio, H. A. D. Q. (2017). Land use impact on soil erosion at different scales in the Brazilian semi-arid. Revista Ciência Agronômica, 48(2), 251-260.

Siddi Raju, R., Sudarsana Raju, G., & Rajsekhar, M. (2018). Estimation of Rainfall-Runoff using SCS-CN Method with RS and GIS Techniques for Mandavi Basin in YSR Kadapa District of Andhra Pradesh, India. Hydrospatial Analysis, 2(1), 1-15p.

Sui, D. Z. (1992). A fuzzy GIS modeling approach for urban land evaluation. Computers, environment and urban systems, 16(2), 101-115.

Sun, X., & Li, F. (2017). Spatiotemporal assessment and trade-offs of multiple ecosystem services based on land use changes in Zengcheng, China. Science of the total environment, 609, 1569-1581.

Wang, X., Zhao, X., Zhang, Z., Yi, L., Zuo, L., Wen, Q., ... & Liu, B. (2016). Assessment of soil erosion change and its relationships with land use/cover change in China from the end of the 1980s to 2010. Catena, 137, 256-268.

Xiao, L., Yang, X., Chen, S., & Cai, H. (2015). An assessment of erosivity distribution and its influence on the effectiveness of land use conversion for reducing soil erosion in Jiangxi, China. Catena, 125, 50-60.

Zohaib, M., Kim, H., & Choi, M. (2019). Detecting global irrigated areas by using satellite and reanalysis products. Science of The Total Environment, 677, 679-691.